Available online at www.sciencedirect.com
ScienceDirect
Journal of Photochemistry and Photobiology A: Chemistry 189 (2007) 329–333
Journal of Photochemistry and Photobiology A:Chemistry
www.elsevier.com/locate/jphotochem

Improved performance of solid-state dye-sensitized solar cells with p/p-type nanocomposite electrolyte

Changneng Zhang *, Kongjia Wang, Linhua Hu, Fantai Kong, Li Guo

Division of Solar Energy Materials and Engineering, Institute of Plasma Physics, Chinese Academy of Sciences, P.O. Box 1126, Hefei, Anhui 230031, PR China

Received 23 September 2006; received in revised form 7 January 2007; accepted 20 February 2007
Available online 23 February 2007

Abstract

A high charge conductivity of p/p nanocomposite PEDOT–PSS/CuI, by in situ deposition of CuI nanocrystals on the surfaces of PEDOT–PSS (poly(3,4-ethylenedioxy-thiophene)–poly(styrenesulphonate)) colloidal nanoparticles has been prepared, for the first time, to fabricate novel solid-state dye-sensitized solar cells. The p-type CuI on the surface of PEDOT–PSS particles and its electrochemical properties were investigated by the transmission electron microscopy (TEM), X-ray photoelectron spectroscopy (XPS) and cyclic voltammetry measurement (CV). The increased charge transport conductivity (σ) and the highest occupied molecular orbital energy levels (E_{HOMO}) were dominated by the p-type CuI in the nanocomposites. By doping CuI in the hole-transporting layer, a noticeable power conversion efficiency has been achieved compared to the solid-state DSCs with PEDOT–PSS, which shown that the p/p-type nanocomposites could be successfully used to construct practical potentials in solid-state DSCs.

Keywords: Hole-transporting materials; Nanocomposites; Dye-sensitized; Solar cell

1. Introduction

The environment-friendly dye-sensitized solar cells (DSCs) have attracted much attention since 1991 [1–4], due to their high efficiency and low production cost for practical applications. The typical DSC is normally in a sandwiched configuration, filled with an organic solution comprising I^-/I_3^- redox couple in the space between the dye-sensitized nanocrystalline TiO_2 photoelectrode and the platinized counter electrode. Under the irradiation of visible light, the dye molecules become photo-excited and ultrafastly inject electrons into the conduction band of TiO_2, then, the oxidized dye sensitizer is effectively scavenged by the redox system which itself is regenerated at the counter electrode by passing electrons through the external load [2]. The effective hole transport in the electrolyte plays an important role in the regeneration of the oxidized dye to get high efficiency for DSCs [5]. However, the problems (e.g., device sealing, solvent evaporation and the cell stability) related to the liquid electrolyte still remain challenges for practical application. Many efforts have been made to replace the liquid electrolyte with solid electrolyte, such as (i) polymers or polymeric/inorganic nanocomposites containing I^-/I_3^- redox couple [6,7], (ii) inorganic p-type semiconductors [8], and (iii) organic hole conductors and hole-transporting polymers [9,10].

Poly(3,4-ethylenedioxy-thiophene), a p-type semiconducting insoluble polymer, exhibits interesting properties, such as high charge conductivity (ca. 300 S/cm), stability and transparency in the visible light region compared to the other hole-conducting polymers [11]. Doping of PEDOT with PSS, resulted in a water-soluble polymer system (PEDOT–PSS) with high charge conductivity, good film-forming properties, high transparency in visible range and excellent stability [11]. Johansson et al. have developed solid-state DSCs by using water-soluble PEDOT–PSS as hole transportor [12], but the open-circuit voltage (V_{oc}) and energy conversion efficiency (η) of this device were significantly lower. The inorganic semiconductors such as water-insoluble and transparent γ-CuI with the band gap ∼3.1 eV, exhibit a high mobility of charge-carriers for solid-state DSCs [13]. Mixing conducting polymers with an inorganic semiconductor can result in a system with an improved

* Corresponding author. Tel.: +86 551 5593222; fax: +86 551 5591377.
E-mail address: solar@ipp.ac.cn (C. Zhang).

1010-6030/$ – see front matter © 2007 Elsevier B.V. All rights reserved.
doi:10.1016/j.jphotochem.2007.02.023

charge-carrier mobility and a combination of the properties of components (e.g., useful functionality and mechanical integrity) [14,15].

In the present work, the p-type CuI on the surfaces of the PEDOT–PSS particles and the electrochemical properties of CuI nanocomposite (PEDOT–PSS/CuI) were investigated by TEM, XPS and cyclic voltammetry measurement (CV), and the performance of the solid-state DSCs was found to show a strong dependence on the electrochemical conductivity and intrinsic energy level of nanocomposites.

2. Experimental

The p/p-type hole-transporting composite of PEDOT–PSS/CuI were synthesized via the reduction of $CuCl_2$ by NaI in Baytron PH solution (PEDOT–PSS) as reported elsewhere [16]. Briefly, $CuCl_2$ solution in ethanol was first added into the PEDOT–PSS solution under stirring at ambient temperature; then NaI solution in ethanol was added 10 min later dropwise into the reaction vessel, followed by stirring for another 30 min. The as-prepared composite solution was applied to cast the layers of solid electrolyte for DSCs, and the γ-phase of CuI nanocrystals in nanocomposites was investigated by XRD [16].

To characterize the morphology of CuI by the transmission electron microscopy (TEM) images obtained by employing a Hitachi H-8000 TEM performing at an accelerating voltage of 200 kV, the as-prepared composite solution was centrifuged at 6000 rpm for 20 min and dried in vacuum at 50 °C for 24 h. And the above separated composite was determined Cu chemical surrounding in CuI nanoparticles by X-ray photoelectron spectroscopy (XPS). The XPS analysis was performed at ambient temperature on an ESCALAB MK2 XPS (VG Scientific, East-Grinstead, UK) with a Mg Kα X-ray source, and the binding energies were referred to the C 1s neutral carbon peak at 284.6 eV [17]. Cyclic voltammetry measurements were carried out at room temperature on an IM6e potentiostat (Zahner, Germany) under N_2 atmosphere, using a classical three-electrode arrangement in 0.1 M of aqueous K_2SO_4 solution that served as supporting electrolyte. The working electrode (1.8 cm^2) was made by depositing a thin solid film on SnO_2:F conducting (FTO) glass sheets, that is, depositing the solid films from the nanocomposites dispersion, and the original Baytron PH solution. A Ag/AgCl electrode (3.0 M of KCl aqueous solution) and a platinum film (2 mm × 6 mm) were used as the reference and counter electrode, respectively. The potential of the working electrode is 0 V versus Ag/AgCl electrode before starting of scanning (the scanning rate: 100 mV/s).

DSCs were assembled in a sandwich configuration. To prepare a photoelectrode, a dense TiO_2 film was first deposited on FTO glass (sheet resistance 20 Ω sq^{-1}) as described elsewhere [18], a TiO_2 colloidal suspension synthesized by sol–gel method [4] was then spin-coated onto the dense TiO_2 film, and the as-treated FTO glass was finally heated in air at 450 °C for 30 min to give a photoelectrode with a porous and nanostructured TiO_2 layer of ∼4 μm in thickness [determined by a profilometer (XP-2, AMBIOS Technology Inc.)]. After cooling to 80 °C, the photoelectrode was immersed in an ethanol solution (0.5 mM) of dye N719 [*cis*-dithiocyanate-*N*,*N*′-*bis*-(4-carboxylate-4′-tetrabutyl-ammonium-carboxylate-2,2′-bipyridine) ruthenium (II)] at room temperature for 12 h. Afterwards, a film (ca. 0.6 μm) of solid electrolyte was spin-coated on the sensitized photoelectrode from the Baytron PH solution or the as-prepared nanocomposite solution. After drying at 100 °C in vacuum for 3 h, the surface of electrolyte layer was additionally spin-coated a thin layer of 1-ethyl-3-methylimidazolium-*bis*-(trifluoromethane slufone) imide (EMITFSI) ionic liquid [10] containing 0.2 M Li[$(CF_3SO_2)_2N$] (LiTFSI) [9] and 0.2 M 4-*tert*-butylpyridine (tBP) [10]. Cell assembly was done by pressing a Pt-sprayed counter electrode against the spin-coated photoelectrode, an external clamp was used to maintain the mechanical integrity of the cell without any further sealing. The photoelectric conversion efficiency of the solid-state DSCs (active area 0.16 cm^2) was measured under an illumination of AM 1.5(100 mW cm^{-2}) which was realized on a solar simulator with a Keithley 2400 source meter controlled by Testpoint software (Changchun Institute of Optics Fine Mechanics and Physics, Chinese Academy of Science, calibrated with standard crystalline silicon solar cell, spectral mismatch was not considered).

3. Results and discussion

The particle size and morphology of CuI in PEDOT–PSS/CuI products was observed by TEM, which was shown in Fig. 1. It is indicated that most of CuI nanoparticles are close to sphericity. Although lots of aggregations can be seen in the microphotograph, some separated particles in this image were still could be seen in the aggregations. The average particle size of nanocrystalline was observed to be in the range of 20–35 nm, and the TEM selected area diffraction pattern (inset to Fig. 1) confirmed that the CuI was γ-phase (fcc), which agreed well with the XRD data [16]. Notably, the TEM selected area diffraction shows more diffuse rings and weak diffraction rings, indicating the presence of amorphous phase in the selected area of the CuI particles

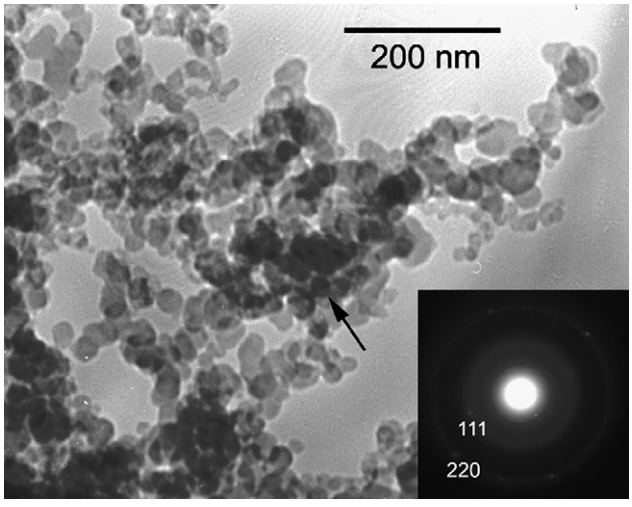

Fig. 1. Transmission electron microscopy (TEM) images of the nanocomposite of PEDOT–PSS/CuI.

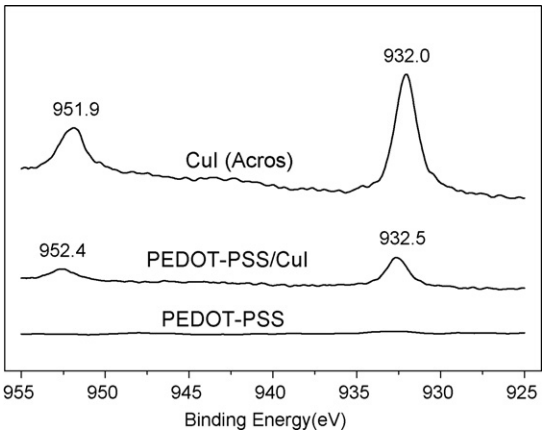

Fig. 2. Cu 2p3/2 XPS spectra of PEDOT–PSS/CuI composites compared with PEDOT–PSS and pure CuI powder (99.995%, Acros).

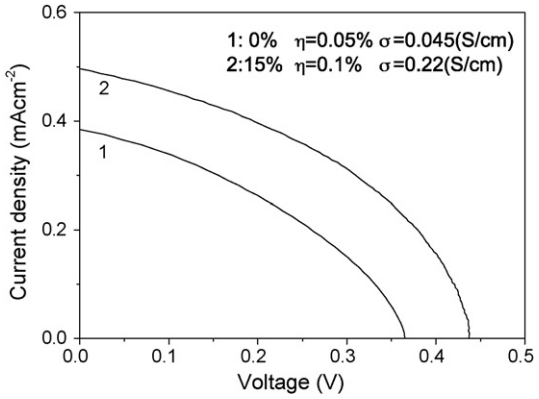

Fig. 3. *J–V* curves of the DSCs based on PEDOT–PSS/CuI (15 wt.%) nanocomposites and original PEDOT–PSS. *Note*: (i) film conductivities (σ) were measured at room temperature by a four-electrode system method after the films were dried in vacuum at 100 °C for 3 h; (ii) the σ value of the PEDOT–PSS film obtained in our experimental conditions was lower than the value of 0.2 (S/cm) from the producer (http://www. hcstarck.com/).

(marked by arrow). Considering the amorphous swollen gel particles of ca. 30 nm in original PEDOT–PSS solution, it is derived that the CuI in our case deposited mainly on the surfaces of those PEDOT–PSS particles. This conclusion can be accounted for the structure of the PEDOT–PSS granular structure that has a higher amount of PSS on the particle surfaces [11,12].

To investigate Cu chemical surrounding in CuI nanoparticles, the XPS signals of PEDOT–PSS/CuI composites were characterized by the Cu 2p3/2 peaks in Fig. 2, The peak of Cu 2p3/2 spectra of the pure CuI powder (99.995%, Acros) is at 932.0 eV in good agreement with the value of 931.9 eV reported for CuI [19], and when reduced Cu^{2+} by I^- in Baytron PH solution, the Cu binding energy in PEDOT–PSS/CuI is increased to 932.5 eV, near to the binding energy of Cu 2p3/2 at 932.7 eV in Cu_2O [20]. The detectable peak shifted to higher binding energy is attributed to Cu species strongly chemisorbed on the surface of PEDOT–PSS for the bond strength of Cu–O in CuI nanocomposites.

Doping of PEDOT with PSS, resulted in a water-soluble polymer system with good film-forming properties. The original PEDOT–PSS film obtained in our experimental conditions has a conductivity of about 0.045 S/cm, and the nanocomposite conductivity could be improved up to 0.22 S/cm by addition of CuI in nanocomposites. Thus, mixing conducting polymers PEDOT–PSS with CuI could result in a system with an improved charge-carrier transport.

In the case of the disordered conducting polymer PEDT–PSS, the charge-carrier mobility is supposed to proceed from tunneling between small conducting grains separated by insulating bar-tiers [21,22]. The deposition of CuI on the surface of PEDOT–PSS could act as bridge between neighboring chains and therefore improve the charge-carrier mobility.

Fig. 3 displays the *J–V* curves of the DSCs with PEDOT–PSS and PEDOT–PSS/CuI nanocomposites as HTMs under 100 mW/cm^{-2} illumination. The cell with nanocomposites shows a short-circuit current (J_{sc}) of 0.50 mA cm^{-2}, an open-circuit voltage (V_{oc}) of 0.44 V, fill factor (FF) of 0.43 and an energy conversion efficiency (η) of 0.1%, higher than those of the cell with only PEDOT/PSS (i.e., $J_{sc} = 0.38$ mA cm^{-2}, $V_{oc} = 0.36$ V, FF = 0.38, $\eta = 0.05\%$). It is obvious that the addition of CuI nanoparticles could improve the cell performance.

The combination of the intrinsic p-type properties of PEDOT–PSS and CuI, could improve the charge transport in the effective regeneration of the oxidized dye to get the high J_{sc} of the solar cells. So the J_{sc} of the cell with nanocomposites is actually due to the improved charge transport conductivity to suppress the recombination at the interface.

The V_{oc} of the solar cells is generally determined by the energy difference between the E_{CB} of TiO_2 and E_{redox} [23]. Although it is not yet very clear whether one should use the E_{ox}, the E_{HOMO} level, or some other energy level for the conducting polymers that is used in DCSs as a hole conductor [12,24]. The lowest unoccupied molecular orbital (LUMO) and the highest occupied molecular orbital (HOMO) energy levels is widely used to describe the thermodynamics of these cells [24,25]. Moreover, in inorganic semiconductor, the maximum valance band (V_B) is regarded to be equal to the HOMO of the p-type material [26]. Thus, in solid-state DSCs with CuI nanocomposites as HTMs, the photovoltage approachable (V_{oc}) is evaluated to be the difference between the E_{CB} of TiO_2 and the E_{HOMO} of the hole conductors.

The cyclic voltammetric behaviours of nanocomposites with p-type CuI on the surfaces of those PEDOT–PSS particles, were investigated by depositing a thin film on FTO glass sheet as shown in Fig. 4. The PEDOT–PSS in original Baytron PH solution exhibited reversible broad oxidation and reduction peaks, similar to the case of PEDOT [27,28] and the PEDOT–PSS film precipitated from Baytron P solution (Bayer AG, solid content 1.2%) or crosslinked by Ca^{2+} ions [29]. According to $E_{HOMO} = -(4.4 + E^0_{ox})$ eV (where, E^0_{ox} versus NHE) [30], the PEDOT–PSS in the original Baytron solution (E^0_{ox} at ~0.35 V versus Ag/AgCl) had E_{HOMO} of −4.97 eV (versus vacuum), close to E_{HOMO} of PEDOT (−5.1 eV) associated to the electron transfer during the oxidation process [27]. In case of CuI, there were two oxidation processes located at 0.04 V and 0.57 V, respectively. The oxidation at 0.57 V (versus Ag/AgCl) or the

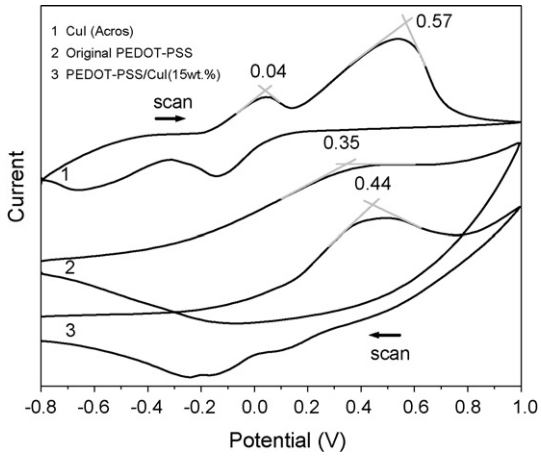

Fig. 4. Cyclic voltammograms of PEDOT–PSS/CuI composites compared with PEDOT–PSS and pure CuI. Scan rate: 100 mV/s.

E_{HOMO} of −5.19 eV (versus vacuum), was in our case assigned to the due of the electron transfer during the oxidation of CuI, which agree with −5.3 eV reported by others [8]. At the beginning of the anodic scanning, the peak at 0.04 V to the oxidation of Cu^+ promoted by water in our experiments was also observed by others during the oxidation of Cu^+/Cu^{2+} couple in a certain amount of water as supporting electrolyte [31]. From the electrochemical properties of the nanocomposites, the two reduction peaks taken for two reduction processes for the nanocomposites, indicated a certain content of PEDOT–PSS in p/p-type CuI nanocomposites; and the broad oxidation peak of the PEDOT–PSS in original Baytron PH solution, exhibited an overlap peak in nanocomposites. Compared with the original PEDOT–PSS, the oxidation peak of the nanocomposites showed a considerable shift to 0.44 V (versus Ag/AgCl) or the E_{HOMO} of −5.04 eV (versus vacuum). This could be explained the electron transfer and redox oxidation of Cu^+ across the surface of nanocomposites faster than that of PEDOT. Thus, the electrochemical property of the nanocomposites was dominated by p-type CuI to improve the E_{HOMO} in the CuI nanocomposites.

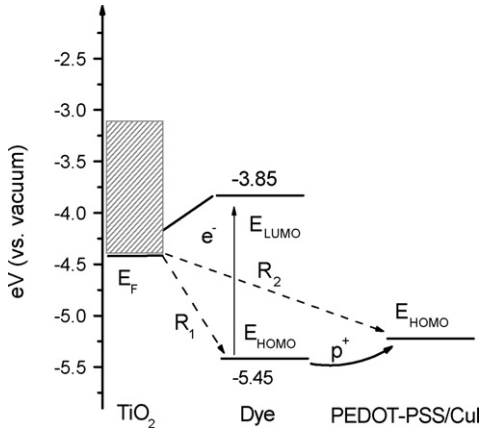

Scheme 1. Energy band diagram of the nanocomposites used in our cell system and the schematic representation of the possible charge transport processes. The solid arrows indicate hole (p^+) flowways, while the dashed arrows are the possible recombination pathways (R_1 and R_2).

From the energy band diagram of the nanocomposite depicted in Scheme 1 in our cell system, it can be seen that the observed V_{oc} of the solid-state cell with nanocomposites was improved due to the increase of E_{HOMO} of the conducting nanocomposite. Under light irradiation, the photo-excited electrons in the molecules were ultrafastly injected into the conduction band of TiO_2, and the higher conductivity of the CuI nanocomposites played an important role in the regeneration of the oxidized dye sensitizers to get high photocurrent (J_{sc}) and in reduction of the ohmic contacts to get high fill factor (FF) for the solid-state DSCs.

In experiments, we also found that the particle size of CuI could remarkably affect the performance of the solid-state DSCs. When the micro meter size of the pure CuI powder (99.995%, Acros) was used instead of the CuI nanocomposite, the performance of the solid-state DSCs decreased dramatically to a short-circuit current (J_{sc}) of 0.07 mA cm^{-2} and an open-circuit voltage (V_{oc}) of 7.7 mV. This could be bad electronic contact leading to the decrease of the observed V_{oc} and J_{sc} of the DSCs with pure CuI powder due to the rapid interfacial charge recombination between the dyed TiO_2 and larger crystal CuI. Compared to DSCs with pure CuI as HTMs, the cell performance was greatly improved by the CuI nanocomposites as HTMs. But in solid-state DSCs with p/p-type nanocomposites, the observed V_{oc} and J_{sc} are well below the cells with liquid electrolyte, due to the severity of recombination at dyed TiO_2/hole conductor interface.

4. Conclusion

In conclusion, for the first time, we described the fabrication of solid-state DSCs based on p/p-type nanocomposites showed a remarkably power conversion efficiency (η) compared to DSCs with PEDOT–PSS. The presence of amorphous CuI phase and Cu species strongly chemisorbed on the surfaces of PEDOT–PSS were investigated by the TEM selected area diffraction and elemental high-resolution electron spectroscopy (XPS) in CuI nanocomposites. The increased charge transport conductivity could suppress the recombination at the interface to increase the J_{sc} of the cell, and the improvement of E_{HOMO} in CuI nanocomposites could improve the potential difference between the E_{CB} of TiO_2 and E_{HOMO} of the HTMs to get the high open voltage (V_{oc}). Further improvement of the photovoltaic performance is expected, to increase the electric contact of the HTMs with the dyed TiO_2 mesoporous film.

Acknowledgement

National Basic Research Program of China (grant no. 2006CB202600) is greatly appreciated for financial supports.

References

[1] B. O'Regan, M. Grätzel, Nature 353 (1991) 737.
[2] M. Nazeeruddin, P. Pechy, T. Renouard, S. Zakeeruddin, R. Humphry-Baker, P. Comte, P. Liska, L. Cevey, E. Costa, V. Shklover, L. Spiccia, G.B. Deacon, C. Bignozzi, M. Grätzel, J. Am. Chem. Soc. 123 (2001) 1613.

[3] J.B. Christophe, F. Arendse, P. Comte, M. Jirousek, F. Lenmann, V. Shklover, M. Grätzel, J. Am. Ceram. Soc. 80 (1997) 3157.
[4] M.K. Nazeeruddin, A. Kay, I. Rodicio, R. Humpbry Baker, E. Miiller, P. Liska, N. Vlachopoulos, M. Grätzel, J. Am. Soc. Chem. 115 (1993) 6382.
[5] S. Nakade, T. Kanzaki, S. Kambe, Y. Wada, S. Yanagida, Langmuir 21 (2005) 11414.
[6] A.F. Nogueira, J.R. Durrant, M.-A. De Paoli, Adv. Mater. 13 (2001) 826.
[7] T. Stergiopoulos, I.M. Arabatzis, G. Katsaros, P. Falaras, Nanoletters 2 (2002) 1259.
[8] K. Tennakone, G.R.R.A. Kumara, I.R.M. Kottegoda, K.G.U. Wijayantha, V.P.S. Perera, J. Phys. D: Appl. Phys. 31 (1998) 1492.
[9] U. Bach, D. Lupo, P. Comte, J.E. Moser, F. Weissörtel, J. Salbeck, H. Spreitzer, M. Grätzel, Nature 395 (1998) 583.
[10] Y. Saito, N. Fukuri, R. Senadeera, T. Kitamura, Y. Wada, S. Yanagida, Electrochem. Commun. 6 (2004) 71.
[11] L. Groenendaal, F. Jonas, D. Freitag, H. Pielartzik, J.R. Reynolds, Adv. Mater. 12 (2000) 481.
[12] E.M.J. Johansson, A. Sandell, H. Siegbahn, H. Rensmo, B. Mahrov, G. Boschloo, E. Figgemeier, A. Hagfeldt, S.K.M. Jönsson, M. Fahlman, Synth. Met. 149 (2005) 157.
[13] A. Konno, T. Kitagawa a, Hiroaki Kida, G.R.A. Kumara, K. Tennakone, Curr. Appl. Phys. 5 (2005) 149.
[14] D.S. Ginger, N.C. Creenham, Phys. Rev. B 59 (1999) 10622.
[15] M. Gao, B. Richter, S. Kirstein, Adv. Mater. 9 (1997) 802.
[16] C. Zhang, M. Wang, F. Li, M. Kong, L. Guo, W. Xu, X. Zhu, K. Wang, Plasma Sci. Tech. 7 (2005) 2962.
[17] S. Wu, E.T. Kang, K.G. Neoh, H.S. Han, K.L. Tan, Macromolecules 32 (1999) 186–193.
[18] A.C. Arango, L. Johnson, V. Bliznyuk, Z. Schlesinger, S.A. Carter, H. Horhold, Adv. Mater. 12 (2000) 1689.
[19] L.M. Engelhardt, P.C. Healy, R.M. Shepherd, B.W. Skelton, A.H. White, Inorg. Chem. 27 (1988) 2371.
[20] A. Losev, K. Kostov, G. Tyuliev, Surf. Sci. 213 (1988) 564.
[21] A.N. Aleshin, S.R. Williams, A.J. Heeger, Synth. Met. 94 (1998) 173.
[22] L. Zuppiroli, M.N. Bussac, S. Paschen, O. Chauvet, L. Forro, Phys. Rev. B 50 (1994) 5196.
[23] D. Cahen, G. Hodes, M. Grätzel, J.F. Guillemoles, I. Riess, J. Phys. Chem. B 104 (2000) 2053.
[24] G.P. Smestad, S. Spiekermann, J. Kowalik, C.D. Grant, A.M. Schwartzberg, J. Zhang, L.M. Tolbert, E. Moons, Sol. Energy Mater. Sol. Cells 76 (2003) 85.
[25] R. Senadeera, N. Fukuri, Y. Saito, T. Kitamura, Y. Wada, S. Yanagida, Chem. Commun. (2005) 2259.
[26] O.-I. Mićić, B.-B. Smith, A.-J. Nozik, J. Phys. Chem. B 104 (2000) 12149.
[27] Q. Pei, G. Zuccarello, M. Ahlskog, O. Inganäs, Polymer 35 (1994) 1347.
[28] S. Garreau, G. Louarn, J.P. Buisson, G. Froyer, S. Lefrant, Macromolecules 32 (1999) 6807.
[29] S. Ghosh, O. Inganäs, Synth. Met. 101 (1999) 413.
[30] L. Wang, M.-K. Ng, L. Yu, Phys. Rev. B 62 (2000) 4973.
[31] M.J. Samide, D.G. Peters, J. Electroanal. Chem. 443 (1998) 95.